Published in IET Electric Power Applications
Received on 12th October 2009
Revised on 11th June 2010
doi: 10.1049/iet-epa.2010.0070

ISSN 1751-8660

Modelling transformer core joints using Gaussian models for the magnetic flux density and permeability

I. Hernández[1,2] *F. de León*[2] *J.M. Cañedo*[1]
J.C. Olivares-Galván[3]

[1]*Departamento de Sistemas Eléctricos de Potencia, CINVESTAV Unidad GDL, Guadalajara, JAL 45015, Mexico*
[2]*Department of Electrical & Computer Engineering, Polytechnic Institute of NYU, Brooklyn, NY 11201, USA*
[3]*Departamento de Energía, Universidad Autónoma Metropolitana, Ciudad de México, DF 02200, Mexico*
E-mail: ihernand@gdl.cinvestav.mx

Abstract: Simple equivalent permeability and reluctance models are obtained for the transformer core joints from the analysis of the magnetic flux. It is shown that the flux variations in the joint zone can be fitted with simple Gaussian expressions suitable for transformer design purposes. These models are derived from 2D and 3D finite element simulations. The magnetic flux distribution in the transformer core joints is studied for wound cores and stacked-lamination cores with step-lap configurations. The models of the study properly account for the effects of core design parameters such as length of air gaps, number of laminations per step and overlap length. The proposed models, which include saturation and anisotropy, are applied to grain-oriented silicon steel (GOSS) and super GOSS. The new models are intended to estimate, right from the design phase, the magnetic flux density, permeability and the reluctance in the joints. The maximum differences between the Gaussian models of this study and finite element simulations are under 6%. The models of this study can be used to improve core designs with the aim of reducing core losses and magnetising current. A comparison of the total losses computed with the model of the study and measurements on a wound core distribution transformer showed differences of about 2.5%.

1 Introduction

Increasingly important in the transformer industry is to reduce the core losses and improve the estimation techniques right from the design stage. With these objectives several studies have been carried out in the last decades [1–18]. Computing the magnetic field distribution inside the core, and particularly at the joints, is essential to estimate the core losses. The joint zone contains the air gaps and overlaps that cause the magnetic field lines to jump to adjacent laminations. This deviation of the magnetic field lines with respect to the rolling direction creates localised regions of higher magnetic flux density and therefore increased losses.

Several papers have analysed the magnetic field distribution in the joint zone. For example, Moses *et al.* [1] and Moses [2] present experimental results for the 'T zone' of three-phase, three-limb transformer cores. A study considering the construction parameters, such as overlap length, air-gap length and the use of step-lap is presented in [3–5]. The influence of these parameters on the magnetic field distribution was first analysed using finite element method (FEM) in [6–10] and circuital models in [11]. In [12–15] it was shown that the core losses are dependent on the instantaneous value of the magnetic field in the laminations, the physical properties of the core material, the operation frequency and the construction parameters of the joint area. In [16, 17] techniques are presented to model the core. In [18] the permeability model in the joints of the step-lap transformer core is included. It has been reported that longitudinal magnetic field distortion greatly influences the core losses. For

example, Pfützner *et al.* [19] present interesting results in 3D studies. Worth noting is that air-gap length, overlap length, number of laminations per step and quality of the material have significant effects in the core losses.

Curve fitting techniques have been used extensively to model ferromagnetic materials' properties; see for example [20–22]. Among others, rational fractions [20], exponentials [21], arctangents [22], step function [23] and power curves [24] have been used. The common feature of all existing curve fitting techniques is that they are applied to represent the material properties: saturation and hysteresis. In this paper we perform curve fitting to characterise the flux density variations along the rolling direction in a transformer core with special emphasis in the joint zone; we assume that the magnetising characteristics of the material are known.

The main contribution of this paper is to provide a simple model to determine the magnetic flux density, permeability and reluctance, properly considering saturation and the anisotropic phenomena in the core joint zone. The new model consists of two exponential terms; therefore it can be easily included in transformer design computer codes. The model offers an accurate and efficient alternative to the more computer intensive FEM. The Gaussian model derived in this paper gives the necessary information to improve the core design by effectively accounting for the complex 3D arrangements of commonly used core joints. The computation of the effects of eddy currents and losses are not within the scope of this paper and are left for a sequel paper. However, for validation purposes, a comparison of the losses computed using our model against experimental results is presented. This shows a difference of about 2.5%.

A large number of finite element simulations are performed to compute the parameters of the model. This is so because the model covers all commonly used ferromagnetic materials for large power transformers. We make the remark that although a large number of finite element simulations were necessary to obtain the model, to use the model in the loop of a design program only requires the evaluation of very simple expressions. This makes the model very efficient, yet it offers comparable accuracy with FEM.

2 Core configurations

Two different designs of transformer cores are studied under no-load conditions: wound core and multi-step lap column core. In this paper, the wound core configuration is used for single-phase transformers, whereas the step-lap column type configuration is used for single- and three-phase transformers; see Figs. 1 and 2.

All core configurations have one or more joints where the magnetic field is not uniformly distributed. The path for the magnetic field in the laminations is commonly represented with non-linear reluctances $\mathcal{R}_L$. A wound core configuration with its magnetic path is shown in Fig. 1*a*. Building the geometric model is very useful to visualise the magnetic field distortion in the overlap and gap zones. Fig. 1*b* shows the construction parameters: overlap length s, air-gap length g, lamination thickness d and number of laminations per step nl.

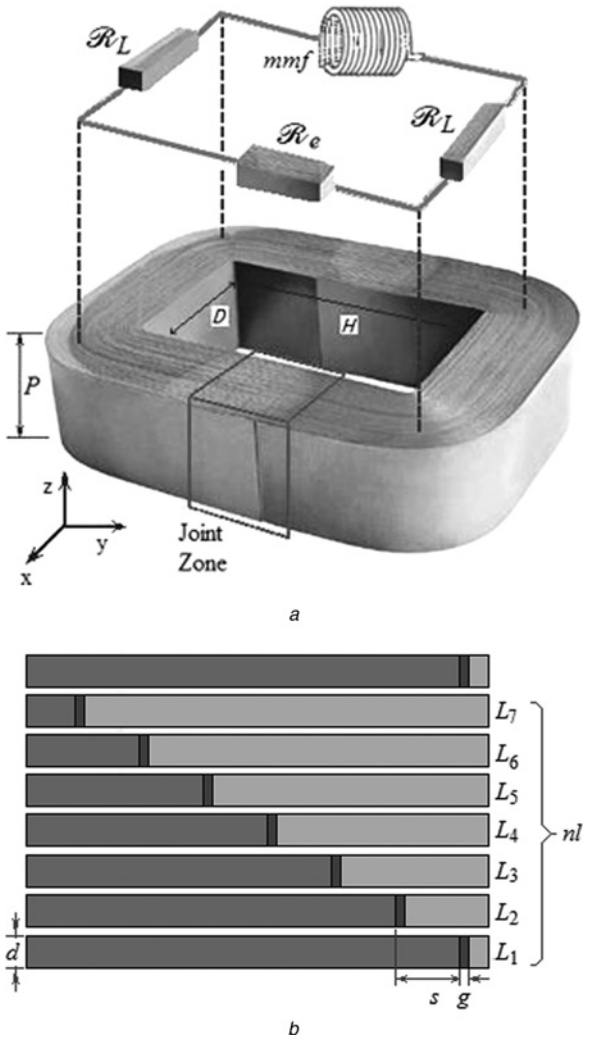

Figure 1 *Wound type core*

a Joint zone and reluctances
b Joint zone with $nl = 6$ laminations per step

Another important core type for transformers is the step-lap core. With this configuration, distribution and power transformers are manufactured. Fig. 2 shows a step-lap core including L and T joint types.

In this paper four of the most common grain-oriented silicon steels (GOSSs) M4 (0.28 mm), M5 (0.3 mm), M6 (0.35 mm), and M5H2 (0.30 mm) are selected for study. The B–H curves for the GOSS used in this paper are taken from [25].

doi: 10.1049/iet-epa.2010.0070

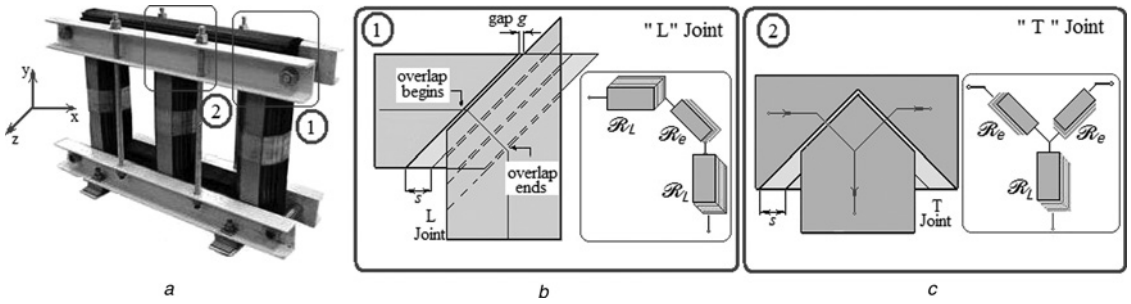

Figure 2 *Step-lap column type core*

a Joint zones
b L joint with its reluctances
c T joint with its reluctances

3 Finite element simulations

The first step for the derivation of the model is the computation of the distribution of the magnetic flux density B in the laminations by finite element simulations in 2D and 3D. We use the general potential formulation given in [7]. We consider the anisotropy of the core laminations. The permeability on the normal direction along the lamination surface is taken as $\mu_r = 10\,000$ as is specified by the manufacturer in [25]. Comparatively, this value is about three times smaller than the permeability of the rolling direction, which varies in accordance with the saturation curve.

All the simulations in this paper were performed using two different commercially available FEM software packages for electromagnetic field analysis. We considered lamination-by-lamination in the analysis. However, full cores were not computed wholly laminated in the 3D analyses because of computer memory limitations. Instead, we simulated groups of up to 36 laminations (for the three-phase column-type cores). These lamination groups were set in different positions until all the laminations in the core were covered. The transformer tank walls were represented by a magnetic insulation boundary because we are not interested in the magnetic fields outside the core.

All the simulations in this paper were performed using two different commercially available FEM software packages for electromagnetic field analysis: COMSOL Multiphysics 3.5a and ANSYS V11. 3D simulations with 36 laminations require approximately 11 GB of memory with 600 000 elements and take less than 30 min to solve in a 12 GB computer Core i7 CPU 2.67 GHz (64 bits operating system). 2D simulations of an entire core consume about 6 GB of memory using close to 800 000 elements and take about 20 min to solve in the same computer.

Fig. 3*a* shows the magnetic flux path along a lamination close to the external edge of the pack. Fig. 3*b* shows, from

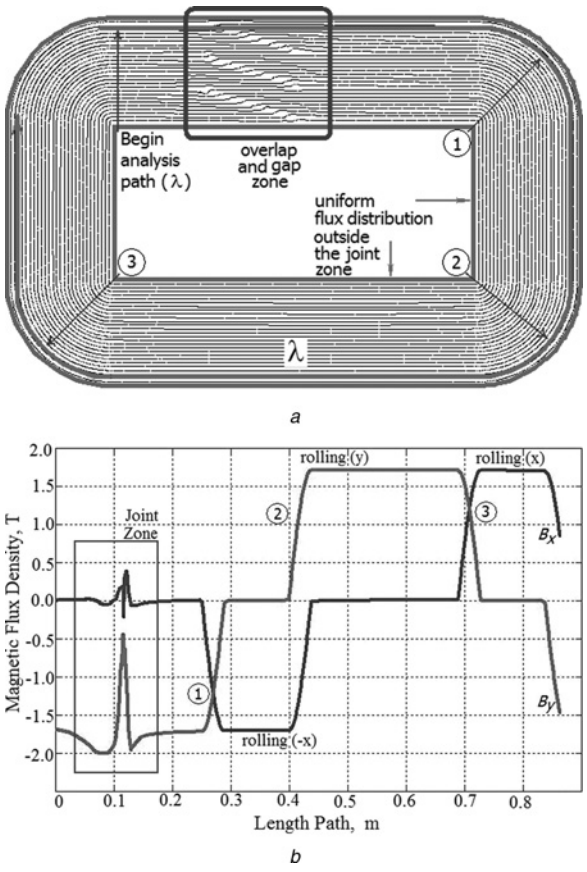

Figure 3 *Magnetic flux density*

a Magnetic path for the analysis of a single-phase wound core. Points 1–3 indicate change in the rolling direction
b Variation of the *x* and *y* components of the magnetic flux density along the path

a 2D FEM analysis, that the magnetic flux follows the rolling direction of the lamination.

From the 3D simulations of an L-joint, presented in Fig. 4, one can note the following: (i) Fig. 4*b* shows that the bulk of the magnetic flux follows the rolling direction; (ii) Fig. 4*c* shows that the z component of the magnetic flux density B_z only exists in the joint zone and (iii) as expected, B_z is very small when it is compared to B_x and B_y.

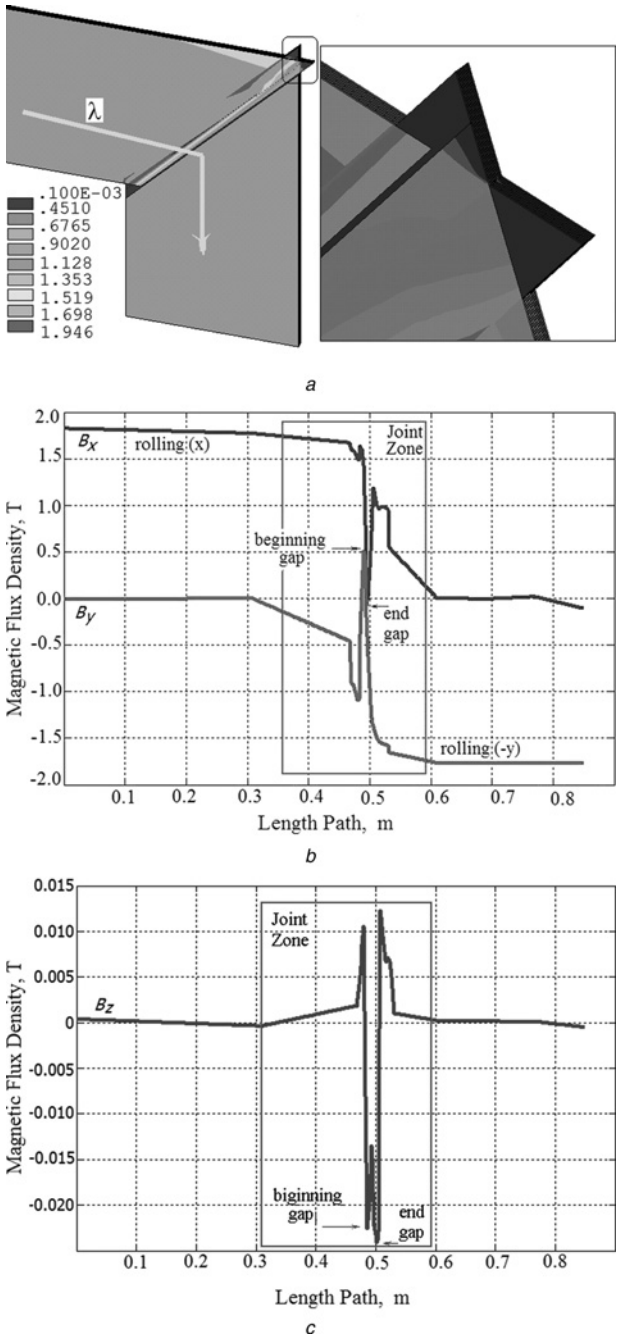

Figure 4 *Magnetic flux density*

a In an L joint of a step-lap column type core
b B_x and B_y components in a path in the centre of the laminations
c B_z in the centre of the lamination

4 Model

In this section Gaussian models are obtained for the reluctance and magnetic flux density in the joint zone. To obtain the model for the magnetic flux distribution, the norm of the magnetic flux density is computed from

$$B(\lambda) = |\boldsymbol{B}_{(x,y,z)}| = \sqrt{B_x^2 + B_y^2 + B_z^2} \tag{1}$$

where λ is the analysis path along the rolling direction; see Figs. 3*a* and 4*a*; λ is considered to pass in the centre of each lamination. Figs. 5*a* and *b* show the magnetic flux density in the joint zone for a wound core and a multi-step lap column core, respectively. One can see that the magnetic flux density in the joint zone, for both wound and step-lap cores, follows a similar distribution pattern. The norm of the magnetic flux density (1) is nearly constant except at the joint region. To fit a model capable of describing the variation of the flux density in the core joints, the curves of Fig. 5 are conveniently divided into five regions delimited by the markings 1–6.

It is possible to obtain a point-by-point model for the relative permeability variations along λ by combining the norm of magnetic flux density with the corresponding norm of the magnetic field intensity $H(\lambda)$ as

$$\mu(\lambda) = \frac{B(\lambda)}{\mu_0 H(\lambda)} \tag{2}$$

The reluctance of a lamination is given by the ratio of the magnetomotive force (mmf) and the magnetic flux ϕ_A through its cross-sectional area A. Mathematically, the

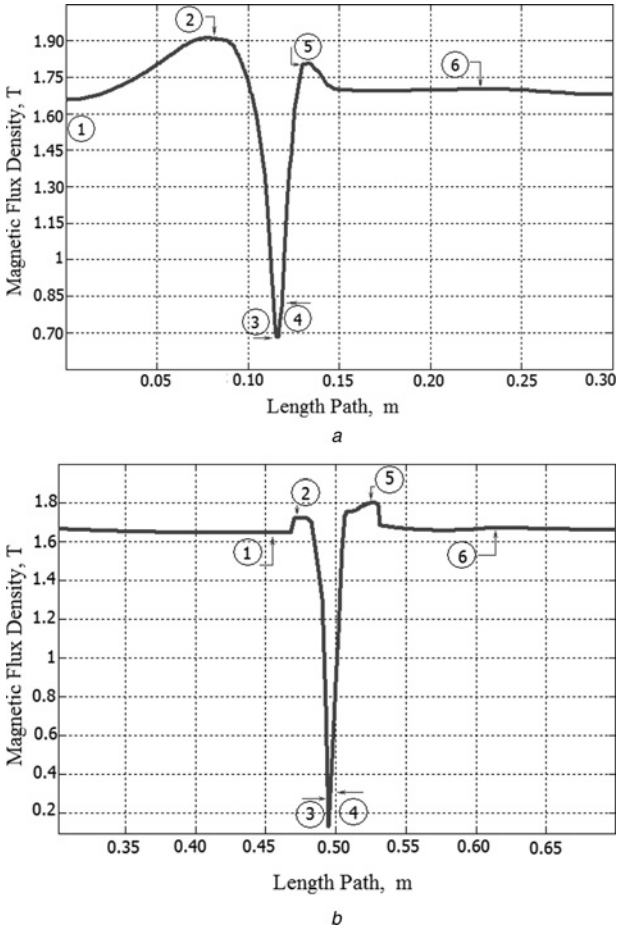

Figure 5 *Magnetic flux density norm*

a In the joint zone of a wound core
b Magnetic flux density norm of L joint

IET Electr. Power Appl., 2010, Vol. 4, Iss. 9, pp. 761–771
doi: 10.1049/iet-epa.2010.0070

reluctance is computed from

$$\mathscr{R} = \frac{\text{mmf}}{\varphi_A} = \frac{\int H\,\mathrm{d}l}{\int B\,\mathrm{d}A} = \frac{l}{\mu_0\mu_R A} \tag{3}$$

Equation (3) is used in the regions where the magnetic flux is constant along the rolling plane direction. However, in the joint zones where the magnetic flux is not constant we need to obtain a reluctance model as function of λ. This can be done with the magnetic flux strength $H(\lambda)$ and the magnetic flux density $B(\lambda)$ obtained point-by-point from the FEM simulations. Therefore the expression for the reluctance in the joint zone becomes

$$\mathscr{R}_e(\lambda) = \frac{\int H(\lambda)\,\mathrm{d}l\,1/B(\lambda)}{\int B(\lambda)\,\mathrm{d}A\,1/B(\lambda)} = \frac{1}{A}\int \frac{\mathrm{d}\lambda}{\mu(\lambda)} \tag{4}$$

where $\mathscr{R}_e(\lambda)$ is the equivalent reluctance in the path λ over the joint zone.

From the observed pattern of magnetic flux density in the joint zone (Fig. 5) we have identified six points that divide the zone into five well-defined regions (Fig. 6) that are amenable for fitting curves. A small region between points 3 and 4, corresponding to the air-gap is included. Modelling this small region is necessary because of the sudden change in permeability from a high value to μ_0 produced by the air gap.

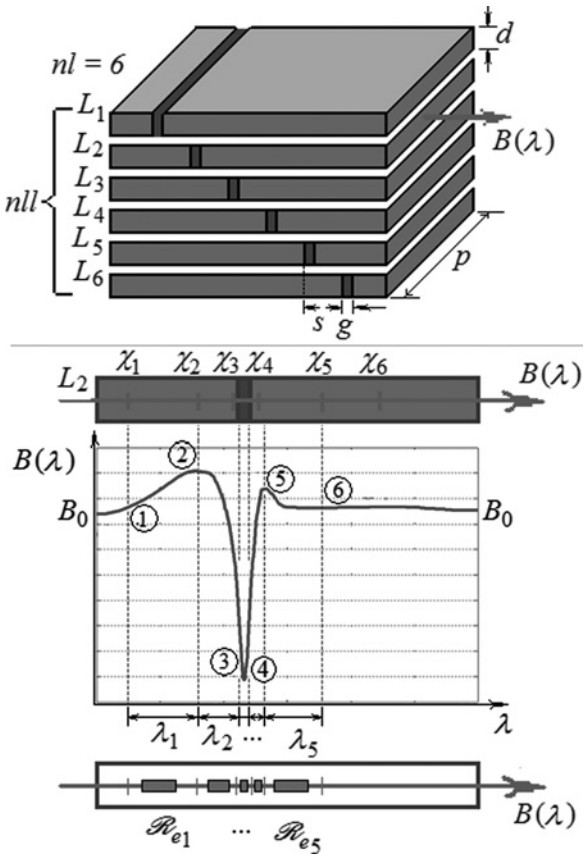

Figure 6 *Parameters needed for the models of the magnetic flux density B(λ) and permeability μ(λ) in the joint zones*

With (4) it is possible to compute the reluctance for each of the five sections in which we have divided the joint zone. To obtain the model we have experimented fitting different functions, for example, polynomials and rational functions gave poor results. Conversely, the Gaussian model offered practical, simple and accurate enough expressions suitable for fitting peaks; see [26, 27].

We propose a Gaussian model to describe the magnetic flux density and the permeability in each section of the joint zone, given by

$$B_i(\lambda) = \alpha_{1,i}\mathrm{e}^{-((\lambda-\beta_{1,i})/\gamma_{1,i})^2} + \alpha_{2,i}\mathrm{e}^{-((\lambda-\beta_{2,i})/\gamma_{2,i})^2} \tag{5}$$

$$\mu_i(\lambda) = \alpha_{3,i}\mathrm{e}^{-((\lambda-\beta_{3,i})/\gamma_{3,i})^2} + \alpha_{4,i}\mathrm{e}^{-((\lambda-\beta_{4,i})/\gamma_{4,i})^2} \tag{6}$$

where $\alpha_{j,i}$ are coefficients related to amplitude; $\beta_{j,i}$ coefficients are related to the position and $\gamma_{j,i}$ are related to the width of the peak. The subscript i represents the section number (from 1 to 5), while j takes values from 1 to 4 [there are four constants in (5) and (6)].

Each section in the joint zone has limiting values χ_i as is shown in Fig. 6. For the initial point of the joint zone, $\chi_0 = 0$. The other χ_i are function of the construction parameters: overlap length s, air-gap length g, lamination thickness d, number of laminations per step nl and the position (or number) that the lamination takes in the pack (nll) where the magnetic flux density or the permeability will be calculated.

For example, to determine the magnetic flux density of the second lamination of a group of six laminations, we use $nl = 6$ and $nll = 2$. The limits χ_i are derived from geometry as

$$\chi_1 = \chi_0 + s(nl - nll) \tag{7a}$$

$$\chi_2 = \chi_1 + nl(2s - g)/2 \tag{7b}$$

$$\chi_3 = \chi_2 + nl(s + g)/3 - g \tag{7c}$$

$$\chi_4 = \chi_3 + 2g \tag{7d}$$

$$\chi_5 = \chi_4 - g + nl(s - g)/2 \tag{7e}$$

$$\chi_6 = \chi_0 + 3(nl)(s) + (s) \tag{7f}$$

4.1 Numerical computation of coefficients α, β and γ

Coefficients α, β and γ in (5) and (6) depend on the following joint construction parameters: overlap length, air-gap length, lamination thickness, number of laminations per step, laminations properties and the cutting angle. A considerable amount of data was generated by performing a large number

of 2D FEM simulations to cover all the design range. About 30% of the simulations were also performed in 3D to validate the 2D model. For a wound core design we have performed 2D (FEM) simulations computing all possible combinations when varying the following design parameters:

1. The overlap length was varied from 5 to 15 mm with steps of 5 mm (three combinations);

2. The number of laminations per step was varied from 2 to 20 in steps of 2 (11 combinations);

3. Lamination properties (B–H curve and thickness) for M4, M5, M6 and M5H2 (four combinations);

4. Flux density from 1.4 to 1.8 T in steps of 0.1 T (five combinations);

5. The air-gap length was varied from 1 to 5 mm in steps of 1 mm (five combinations).

For a step-lap core, in addition to the above combinations, we also varied the cutting angle from 30 to 45° in steps of 5° (giving three extra combinations).

Coefficients α, β and γ are computed for each combination described above. Fig. 7*a* shows the variation pattern of coefficient $\alpha_{1,1}$ (representing the amplitude of the first exponential of the first section) for $nl = 10$ when varying the design magnetic flux density from 1.5 to 1.8 T. Fig. 7*b* shows the variation of $\alpha_{1,1}$, inside a pack of 20 laminations per step when the design flux density is varied as before. Fig. 7(*c*) shows the variation pattern of $\alpha_{1,2}$, (representing the amplitude of the first exponential of the second section) varying the number of laminations per step. Fig. 7(*d*) shows the behaviour of $\alpha_{1,4}$ (the amplitude of the first exponential of the fourth section) for $nl = 8$. One can see from Fig. 7 that the $\alpha_{j,i}$ coefficients follow relatively regular patterns. This makes them suitable for fitting curves. Coefficients $\beta_{j,i}$, represent position in the Gaussian model and therefore depend on the limits χ_i. The $\gamma_{j,i}$

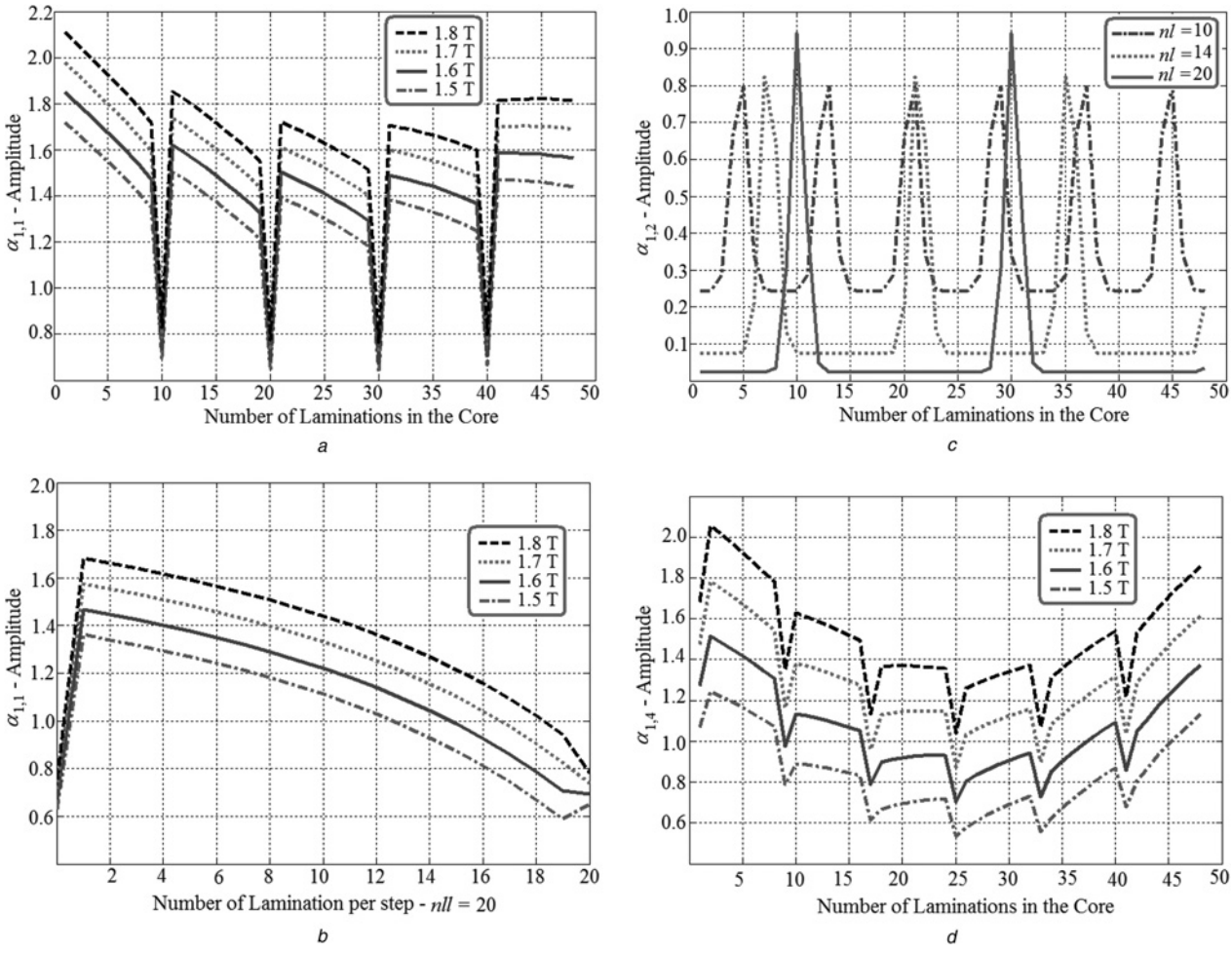

Figure 7 *Behaviour of patterns for different α coefficients*

a $\alpha_{1,1}$ (the amplitude of the first exponential of the first section) for the case when $nl = 10$ while varying B_0
b $\alpha_{1,1}$ for $nl = 10$ varying B_0
c $\alpha_{1,2}$ (amplitude of the first exponential of the second section) varying nl
d $\alpha_{1,4}$ (amplitude of the first exponential of the fourth section) for $nl = 8$ varying B_0

doi: 10.1049/iet-epa.2010.0070

coefficients are constant or function of the overlap (s) and the gap length (g).

4.2 Curve fitting for coefficients $\alpha_{j,i}$

Since we are interested in obtaining formulas to compute $\alpha_{j,i}$ amenable for a transformer design program, we performed least-squares curve fittings to the large amount of data generated above. In this way the $\alpha_{j,i}$ can be easily programmed and there is no need to use large look-up tables. The best curve is fitted to the coefficients $\alpha_{j,i}$ with MATLAB's *curve fit tool* that minimises the error. The results are shown in Table 1 for the flux density model (5) and in Table 2 for the permeability model (6).

One can observe that the values of coefficients $\alpha_{j,i}$ for the magnetic flux density model very much depend on the design magnetic flux density (B_0) and on the peaks (B_{p2}, B_{p5}) and valleys (B_{mn}) of the flux density variation in the joint zone; see Fig. 8. The peaks and valleys are computed from curve fitting yielding:

For peak 2

$$B_{p2} = 1.2707B_0 e^{0.0041nl} - 0.2203e^{0.0854nl} \tag{8}$$

For peak 5

$$B_{p5} = 1.2707B_0 e^{0.007264(n+1)-0.0105nl} - 0.2203e^{0.08858(n+1)-0.0918nl} \tag{9}$$

For valleys 3 and 4

$$B_{mn} = B_{p3} = B_{p4} = \left(1 - \frac{1}{nl} - 1.186e^{-0.198nl}\right) \times e^{-(nll-1-(nl)/2.2)^2} + 1.186e^{-0.198nl} \tag{10}$$

Similarly for the permeability model the $\alpha_{j,i}$ coefficients are function of the design peak and valley permeabilities, the $\beta_{j,i}$ coefficients depend on the position and the $\gamma_{j,i}$ coefficients are constant or function of the overlap (s) and the gap length (g). The peaks and valleys are computed from curve fitting yielding

$$\mu_{p2} = 3.533 \times 10^{-5} e^{0.3112nl} + 3.278 \times 10^{-5} e^{-1.446nl} \tag{11}$$

For peak 5

$$\mu_{p5} = 3.533 \times 10^{-5} e^{0.3112(n-nl+1)} + 3.278 \times 10^{-5} e^{-1.446(n-nl+1)} \tag{12}$$

For valleys close to the air-gap there are small values of B but large values of H, we found that $\mu_n = 0.05623$. The initial (or design permeability) μ_d is computed from the relation between B_0 and H_0 extracted from the B–H curves. The details of the computation of coefficients α, β and γ are given in the flowchart diagram of Fig. 9.

Table 1 Coefficients for the magnetic flux density model (5)

i	λ_i	$\alpha_{1,i}$	$\beta_{1,i}$	$\gamma_{1,i}$	$\alpha_{2,i}$	$\beta_{2,i}$	$\gamma_{2,i}$
1	$\chi_1 \le \lambda_i \le \chi_2$	$B_{p2} - B_0$	χ_2	s	B_0	1	100
2	$\chi_2 \le \lambda_i \le \chi_3$	$-B_{s1} + B_{mn}$	χ_3	$0.5s$	B_{s1}	1	100
3	$\chi_3 \le \lambda_i \le \chi_4$	g	χ_3	g	G	χ_4	g
4	$\chi_4 \le \lambda_i \le \chi_5$	$-B_{p5} + B_{mn}$	χ_4	s	B_{p5}	1	100
5	$\chi_5 \le \lambda_i \le \chi_6$	$B_{s4} - B_0$	χ_5	$2s$	B_0	1	100

Table 2 Coefficients for the permeability model (6)

i	λ_i	$\alpha_{3,i}$	$\beta_{3,i}$	$\gamma_{3,i}$	$\alpha_{4,i}$	$\beta_{4,i}$	$\gamma_{4,i}$
1	$\chi_1 \le \lambda_i \le \chi_2$	μ_d	χ_1	ns	μ_{p2}	1	100
2	$\chi_2 \le \lambda_i \le \chi_3$	μ_g	χ_3	$6g$	μ_{s1}	1	100
3	$\chi_3 \le \lambda_i \le \chi_4$	μ_{s2}	χ_3	10^{-4}	μ_g	χ_4	10^{-4}
4	$\chi_4 \le \lambda_i \le \chi_5$	μ_{s3}	χ_4	Ng	μ_{p5}	1	100
5	$\chi_5 \le \lambda_i \le \chi_6$	$\mu_{s4} - \mu_d$	χ_5	S	μ_d	1	100

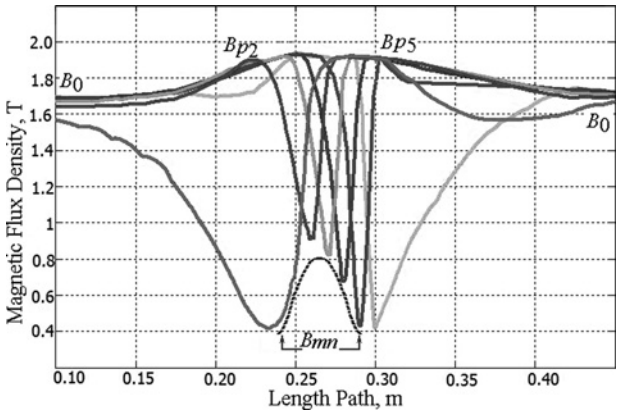

Figure 8 *Family of curves of the magnetic flux density with nl = 6 by step for a wound core*

B_{p2}, and B_{p5} peaks of the magnetic flux density before and after the air-gap, respectively and B_{mn} are valleys in the air-gap

4.3 Losses

To compute the eddy current losses in the region where the magnetic flux density is uniform (most of the lamination length, but excluding the joint zone), we use the classic formulation given by [28]

$$P_{ek} = \frac{1}{24}\sigma(2\pi f)^2 d^3 p L B_k^2 \tag{13}$$

where P_{ek} (W) is the Eddy current losses in the kth lamination, f (Hz) is the operation frequency, σ (S/m) is the lamination conductivity, d (m) is the lamination thickness, p (m) is the lamination width, L (m) is the lamination length and B_k (T) is the average magnetic flux density in the lamination.

At the joint zone where the magnetic field is not uniform we use our model to compute the magnetic flux density. The Gaussian model (5) provides the magnetic flux density at each point of the joint zone for each lamination: $B_k(\lambda)$. To compute the point-by-point losses in the joint zone we modify (8) as follows

$$P_{ek} = \frac{1}{24}\sigma(2\pi f)^2 d^3 p (B_k(\lambda))^2 L j_k \tag{14}$$

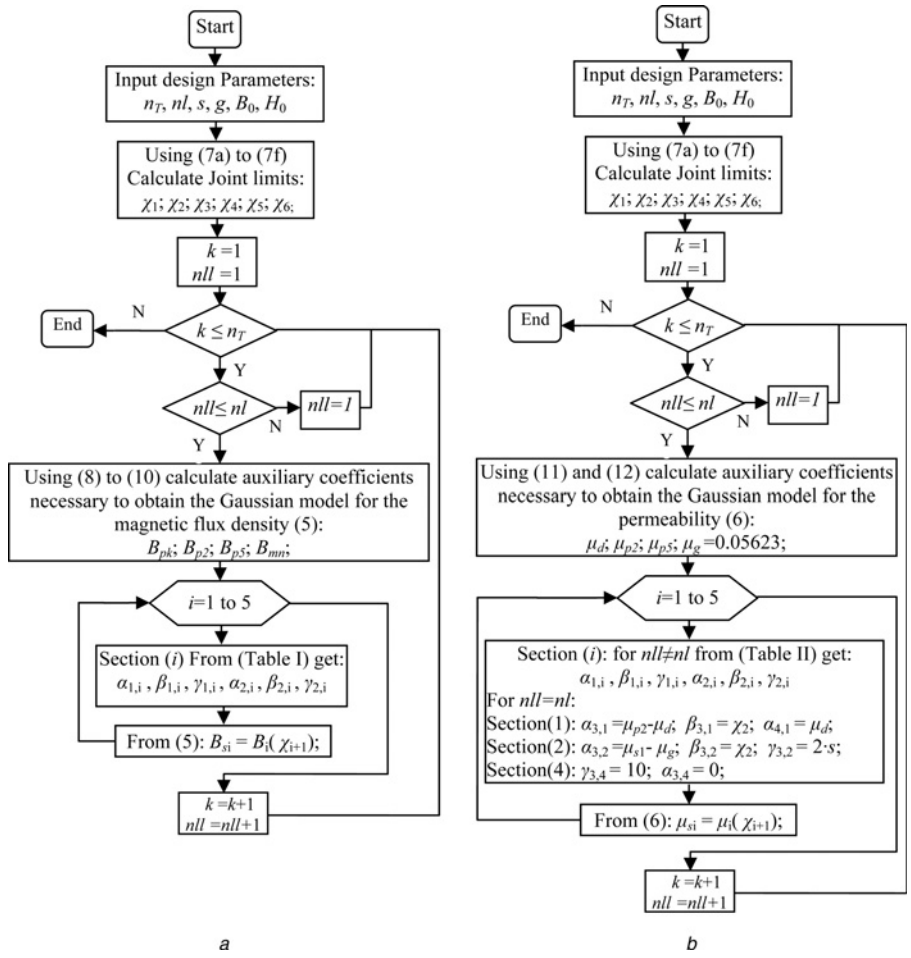

Figure 9 *Flowchart diagram*

a To determine the coefficients in the Gaussian model for B (5)
b Data flowchart diagram to determine the coefficients in the Gaussian model for μ (6)

IET Electr. Power Appl., 2010, Vol. 4, Iss. 9, pp. 761–771
doi: 10.1049/iet-epa.2010.0070

where $B_k(\lambda)$ is the magnetic flux density value obtained point-by-point on the joint zone with length Lj, for the kth lamination.

The Gaussian model for the permeability is used to compute the excitation current drawn by the core. For wound cores, the expressions for the reluctance of each lamination $\mathcal{R}_{ek}$, (3) and (4), can be used to compute an equivalent reluctance of full core $\mathcal{R}_{ec}$. Since the laminations are in parallel, the equivalent reluctance is computed as the inverse of the sum of the inverse reluctances of the individual laminations. Thus the excitation current in amperes per turn is given by

$$I_{exc} = \frac{B_m A_c L_{mc}}{\mathcal{R}_{ec}} \tag{15}$$

where B_m (T) is the average magnetic flux density in the core, A_c (m^2) is the core cross-sectional area and L_{mc} (m) is the core mean length.

5 Validation

5.1 Comparison of the Gaussian model versus FEM

A point-by-point comparison between the calculations using FEM and the model proposed in this paper was performed. The magnetic flux density and the permeability in the joint zone were determined for the two different core configurations. We varied the number of laminations per step from 2 to 20, the overlap distance from 5 to 15 mm and the gap length from 1 to 5 mm. We varied the magnetic flux density B_0 from 1.4 to 1.8 T. The results between the Gaussian model and the FEM calculations are very close. The differences are smaller than 6%. Figs. 10 and 11 illustrate the results for a wound core transformer with $s = 10$ mm, $g = 1$ mm, $nl = 6$ and $nll = 3$.

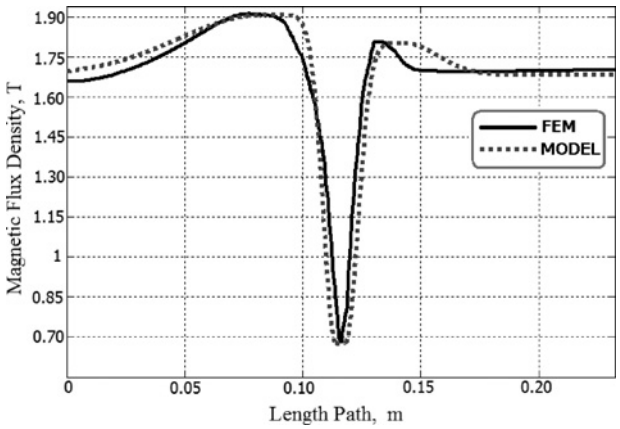

Figure 10 *Comparison between the results of FEM and the approximate model for the magnetic flux density B(λ) with nl = 6 and nll = 3 in a wound core*

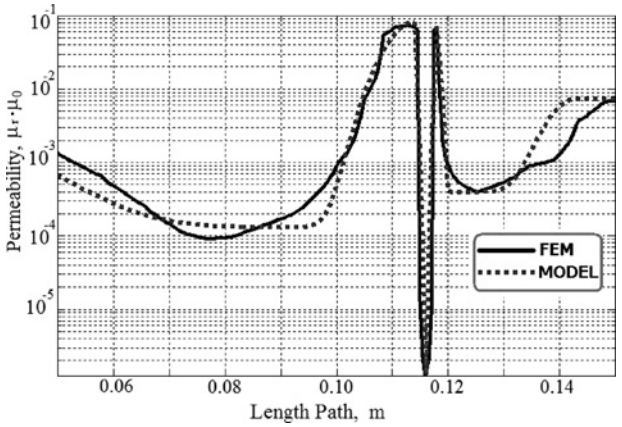

Figure 11 *Comparison between the results of FEM and the approximate model for the permeability point-by-point μ(λ) with nl = 6 and nll = 3 in a wound core*

Results for the L-type joint with different number of laminations are shown in Fig. 12. Again, the largest difference is less than 6% and occurs in the permeability model close to points 2 and 5 of Fig. 5. The reason is that in between those points we have the air-gap where there is a sudden change from high permeability to μ_0. A slightly larger difference (9%) occurs with the external laminations of a group because their characteristics are different to the other laminations; this difference, however, has been proven to have a negligible effect on the overall performance of the model.

GOSS M5 (0.30 mm) was used for the comparisons illustrated in this section. However, similar results have been obtained with our models (5) and (6) for other commonly used transformer steels such as M4 (0.27 mm) and M6 (0.35 mm). Good results were also obtained with super-oriented electrical steel such as M5H2 (0.30 mm).

5.2 Loss measurements

To validate the model we measured the eddy current losses of a wound core distribution transformer. The physical and design characteristics are (Fig. 1 shows the construction parameters): window width $D = 110$ mm; limb width $E = 30.24$ mm; window height $H = 251$ mm; lamination width $P = 190.5$ mm; lamination thickness $d = 0.3$ mm; overlap length $s = 10$ mm; gap length $g = 1$ mm; number of laminations per step $nl = 10$; design flux density $B_o = 1.7$ T. This distribution transformer was manufactured using M5 GOSS operating at 60 Hz. The total core losses measured were 84.12 W. After separating the eddy current losses from the hysteresis and excess losses using the procedure given in [29], we have $W_{eddy(test)} = 19.28$ W, hysteresis losses 22.73 W (using 0.00374 W/lb/cycle, from [25]) and the excess losses are 42.25 W.

Form the FEM simulation we obtain $W_{eddy(FEM)} = 19.71$ W and using our model ((5) together with (14)), we obtain

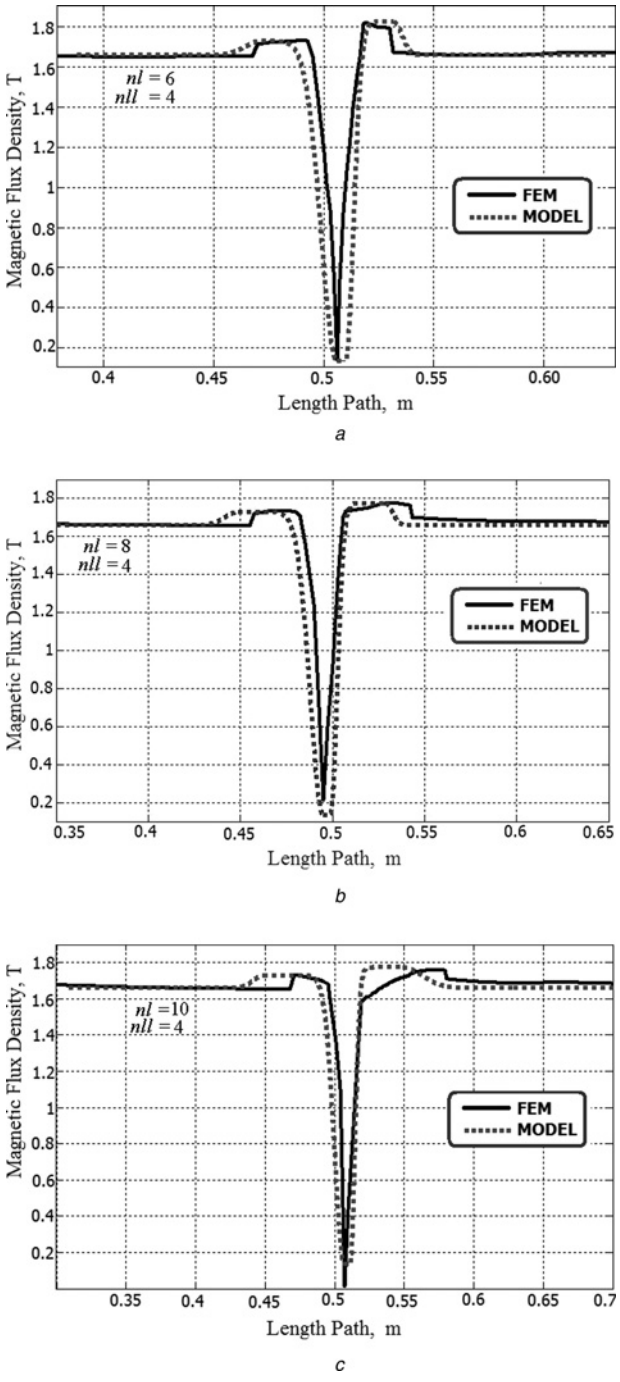

Figure 12 *Magnetic flux density in the L joint*

a With $nl = 6$ and $nll = 4$
b With $nl = 8$ and $nll = 4$
c With $nl = 10$ and $nll = 4$

$W_{\text{eddy(model)}} = 20.23$ W, which represents a relative difference of 2.58% with respect to measurements.

6 Conclusions

Gaussian models for the representation of the variation of the magnetic flux density and permeability along the transformer core joints have been obtained. The models have been derived from numerous 2D and 3D FEM simulations using two different commercial FEM software packages. Note, however, that to use the models only the evaluation of very simple expressions is needed. This makes the model suitable for implementation in the design process loop. The validation was made with a large number of FEM simulations and measurements on a real transformer.

We have found a simple and accurate model by fitting a Gaussian equation for the variation of the magnetic flux density and the permeability in the joint zone. The new permeability and flux density models are functions of the design parameters of the core joints: overlap length, air-gap length, number of laminations per step, lamination properties, and the cutting angle. The benefit of the proposed models is that (5) and (6) can be easily included in transformer design computer programs. Additionally, the CPU time consumed is negligible when compared with 2D or 3D FEM simulations while yielding similar results.

7 References

[1] MOSES A.J., THOMAS B., THOMPSON J.E.: 'Power loss and flux density distributions in the T-Joint of a three phase transformer core', *IEEE Trans. Magn.*, 1972, **8**, pp. 785–790

[2] MOSES A.J.: 'Comparison of transformer loss prediction from computed and measured flux density distribution', *IEEE Trans. Magn.*, 1998, **34**, pp. 1186–1188

[3] LÖFFLER F., BOOTH T., PFÜTZNER H., BENGTSSON C., GRAMM K.: 'Relevance of step-lap joints for magnetic characteristics of transformers cores', *IEE Proc. Electr. Power Appl.*, 1995, **142**, (6), pp. 371–378

[4] VALKOVIC Z.: 'Influence of transformer core design on power losses', *IEEE Trans. Magn.*, 1982, **18**, pp. 801–804

[5] DAUT I., MOSES A.J.: 'Some effects of core building on localized losses and flux distribution in a three phase transformer core assembled from power core strip', *IEEE Trans. Magn.*, 1990, **26**, pp. 2002–2004

[6] ZIENKIEWICZ P.C., LYNESS J., OWEN D.R.: 'Three dimensional magnetic field determination using a scalar potential a finite element solution', *IEEE Trans. Magn.*, 1977, **13**, pp. 1649–1656

[7] GYMESI M., LAVERS D., PAWLAK T., OSTERGAARD D.: 'Application of the general potential formulation', *IEEE Trans. Magn.*, 1993, **29**, pp. 1345–1347

[8] NAKATA T., TAKAHASHI N., KAWASE Y.: 'Magnetic performance of step lap joints in distribution transformer cores', *IEEE Trans. Magn.*, 1982, **18**, pp. 1055–1057

[9] NAKATA T., TAKAHASHI N., FUJIWARA K., SHIRAKI Y.: '3-D magnetic field analysis using special elements', *IEEE Trans. Magn.*, 1990, **26**, pp. 2379–2381

doi: 10.1049/iet-epa.2010.0070

[10] RAIZER A., DEDULLE J.M., MEUNIER G.: 'Magnetic field computation in a transformer core with an automatic adaptive mesh generator', *IEE J. Appl. Phys.*, 1990, **67**, (9), pp. 5806–5808

[11] ELLEUCH M., POLOUJADOFF M.: 'New transformer model including joint air gaps and lamination anisotropy', *IEEE Trans. Magn.*, 1998, **34**, pp. 3701–3711

[12] GIRGIS R.S., TENIJENHUIS E.G., GRAMM K., WRETHAG J.E.: 'Experimental investigations on effect core production attributes on transformers core loss performance', *IEEE Trans. Magn.*, 1998, **13**, pp. 526–531

[13] TENYENHUIS E.G., GIRGIS R.S., MECHLER G.F.: 'Others factors contributing to the core loss performance of power and distribution transformers', *IEEE Trans. Magn.*, 2001, **16**, pp. 648–653

[14] MECHLER G.F., GIRGIS R.S.: 'Magnetic flux distributions in transformers core joints', *IEEE Trans. Power Deliv.*, 2000, **15**, pp. 198–203

[15] TENYENHUIS G.F., GIRGIS R.S.: 'Measured variability of performance parameters of power & distribution transformers'. Proc. IEEE PES Transmission and Distribution Conf. on Exposition, 2006, pp. 523–528

[16] LIEW M.C., BODGER P.S.: 'Partial-core transformer design using reverse modelling techniques', *IEE Proc. Electr. Power Appl.*, 2001, **148**, (6), pp. 513–519

[17] GUERRA F.C.F., MOTA W.S.: 'Magnetic core model', *IET Sci., Meas. Technol.*, 2007, **1**, (3), pp. 145–151

[18] HIHAT N., NAPIERALSKA-JUSZCZAK E., LECOINTE J.PH., SYKULSKI J.K.: 'Computational and experimental verification of the equivalent permeability of the step-lap joints of transformer cores'. IET Seventh Conf. Int. on Computation in Electromagnetics CEM 2008, Brighton, UK, 7–10 April 2008, pp. 38–39

[19] PFÜTZNER H., BENGTSSON C., BOOTH T., LÖFFLER F., GRAMM K.: 'Three dimensional flux distributions in transformers cores as a function of package design', *IEEE Trans. Magn.*, 1994, **30**, pp. 2713–2727

[20] WILDGER G.F.T.: 'Representation of magnetisation curves over extensive range by rational-fraction approximations', *IEE Proc.*, 1969, **116**, pp. 156–160

[21] EL-SHERBINY M.K.: 'Representation of the magnetization characteristic by a sum of exponentials', *IEEE Trans. Magn.*, 1973, **9**, pp. 60–61

[22] PEREZ-ROJAS C.: 'Fitting saturation and hysteresis via arctangent functions', *IEEE Power Eng. Rev.*, 2000, **20**, pp. 55–57

[23] O'KELLY D.: 'Impact and transient excitation of magnetic plate including hysteresis and eddy-current action', *IEE Proc. Sci., Meas. Technol.*, 1992, **139**, (3), pp. 99–106

[24] LUCAS J.R., MCLAREN P.G., KEERTHIPALA W.W.L., JAYASINGHE R.P.: 'Improved simulation models for current and voltage transformers in relay studies', *IEEE Trans. Power Deliv.*, 1992, **7**, pp. 152–159

[25] AK Steel Oriented and TRAN-COR H Electrical Steels, Armco Inc., 2000

[26] BROWN R.: 'All peaks aren't Gaussian', *Pers. Eng. Instrum. News*, 1991, pp. 51–54

[27] GURLEY K.R.: 'Numerical methods lecture 5: Curve fitting techniques'. CGN-3421 computer methods, 2003, pp. 89–102

[28] AGARWAL P.D.: 'Eddy-current losses in solid and lamination iron', *AIEE*, 1959, **78**, pp. 169–181

[29] ZIRKA S.E., MOROZ Y.I., MARKETOS P., MOSES A.J.: 'Loss separation in nonoriented electrical steels', *IEEE Trans. Magn.*, 2010, **46**, pp. 286–289